Journal of Luminescence 227 (2020) 117553

Contents lists available at ScienceDirect

Journal of Luminescence

journal homepage: http://www.elsevier.com/locate/jlumin

Superlinearity revisited: A new analytical equation for the dose response of defects in solids, using the Lambert W function

Vasilis Pagonis [a,*], George Kitis [b], Reuven Chen [c]

[a] McDaniel College, Physics Department, Westminster, MD, 21157, USA
[b] Aristotle University of Thessaloniki, Physics Department, Nuclear Physics and Elementary Particles Physics Section, 54124, Thessaloniki, Greece
[c] Raymond and Beverly Sackler School of Physics and Astronomy, Tel Aviv University, Tel Aviv, 69978, Israel

ARTICLE INFO

Keywords:
Luminescence models
Superlinearity
Nonlinear dose response
Lambert function W

ABSTRACT

In a recent paper we developed a new analytical equation for the dose response of dosimetric materials based on the Lambert W function, within the framework of the simplest model, the one trap one recombination center model (OTOR). In the present paper we extend this recent work to develop a new analytical equation describing the nonlinear trap filling process during irradiation of insulators. The new equations are developed within the framework of a more complex two trap and one recombination center model (2T1R). The model has been proposed previously to explain the nonlinear dose response function of luminescence signals in solids, and is based on competition between two traps during irradiation. The new analytical equation describes the superlinear behavior commonly exhibited by dosimetric materials and contains meaningful physical parameters. It is tested by fitting previously published dose response curves for dosimetric materials.

1. Introduction

The dose response of natural and man-made materials is the basis of many applications in radiation dosimetry. It is commonly shown as a graph of the intensity of an experimentally measured signal as a function of the irradiation dose. Examples of such dosimetric signals are thermoluminescence (TL), isothermal thermoluminescence (ITL), optically stimulated luminescence (OSL), optical absorption (OA) and electron spin resonance (ESR). A desirable feature for these graphs is that the dose dependence be linear in a broad range. However, dosimetric materials show many different types of dose response curves. Nonlinear dose response curves are broadly classified as *superlinearity* (or *supralinearity*), meaning a faster than linear dependence on the dose, and *sublinearity* meaning a lower than linear dose dependence. Some examples of dose responses are: superlinear behavior from very low doses, linear behavior at low doses becoming superlinear at higher doses, sublinear dose dependence from the lowest doses, and linear and/or superlinear range followed by sublinear behavior reaching a saturation level. For a detailed bibliography on dose response functions of thermally and optically stimulated luminescence signals and the various published models, the reader is referred to the books by Chen and Pagonis [1], Yukihara and McKeever [2], Chen and McKeever [3] and McKeever [4].

In the literature, the term superlinearity (or supralinearity) has been quantified using two different types of indexes, the supralinearity index $f(D)$ and the superlinearity index $g(D)$. If the signal intensity is I, one way of presenting the experimental dose response function at low doses, is by the expression (see e.g. Ref. [1]):

$$I_{max} = aD^k \tag{1}$$

where D is the applied dose, a is a proportionality factor and k a constant. $k > 1$ means that the dependence is superlinear whereas $k < 1$ means sublinearity, and obviously $k = 1$ means a linear dependence. Chen and McKeever [5] proposed the quantitative normalized *superlinearity index* $g(D)$, which would attain the value of k in the special case in Eq. (1). They defined $g(D)$ as:

$$g(D) = \frac{DS''(D)}{S'(D)} + 1. \tag{2}$$

Here the condition $g(D) > 1$ indicates superlinearity, $g(D) = 1$ means a range of linearity and $g(D) < 1$ signifies sublinearity.

Some materials (like $LiF : Mg, Ti$) have the property that at low doses the dose dependence is linear, followed by a nonlinear (i.e., superlinear) region before saturation effects set in. Chen and McKeever [5] suggested

* Corresponding author.
E-mail address: vpagonis@mcdaniel.edu (V. Pagonis).

https://doi.org/10.1016/j.jlumin.2020.117553
Received 23 May 2020; Received in revised form 2 July 2020; Accepted 27 July 2020
Available online 6 August 2020

the term *supralinearity* to describe this property of the measured quantity being above the continuation of the initial range. Some authors, e.g. Horowitz [6] and Mische and McKeever [7] quantified this property by defining the dimensionless quantity:

$$f(D) = \frac{S(D)/D}{S(D_1)/D_1}, \tag{3}$$

termed by these authors the *supralinearity index*. Here D_1 is a normalization dose in the initial linear range. This definition is obviously applicable only if an initial linear range exists at the low dose range.

From a modeling point of view, there are very few analytical equations available in the literature to describe the nonlinear dose response function of dosimetric materials. The simplest available model based on delocalized energy transitions is the one trap one recombination center model (OTOR). Previous modeling research has shown that within the OTOR model, one expects an initial linear dose response region for low doses, followed by a sublinear region in which the dose response function varies as $D^{1/2}$, before approaching saturation (Lawless et al. [8]).

Even though the OTOR model has been studied extensively during the past 50 years, it was only recently that Pagonis et al. [9] obtained an *analytical* equation for the dose response $n(D)$ in the OTOR model, where n is the concentration of filled traps and D is the irradiation dose. The new analytical equation for $n(D)$ is based on the well-known Lambert function W ([10,11]). Pagonis et al. [9] compared the new OTOR equation with three other commonly used dose response fitting functions: the saturating exponential (SE), the saturating exponential plus a linear function (SEL), and the double saturating exponential (DSE). These authors provided examples of using the new equation to fit a variety of experimental TL, OSL, ITL and ESR data.

In this paper we extend the recent work by Pagonis et al. [9], into the more general two trap one recombination center model (2T1R). Bowman and Chen [12] developed a*n implicit parametric* equation $D(n)$ within the 2T1R model, where D (Gy) is the irradiation dose and n (cm^{-3}) is the concentration of filled dosimetric traps. This parametric equation $D(n)$ must be inverted numerically to yield the dose response function $n(D)$.

The overall purpose of the present work is to derive a new analytical expression $n(D)$ for the dose response curves in the irradiation stage of the 2T1R model, by using the Lambert function W. The specific goals of this paper are:

- To develop the new analytical equation in the useful form $n(D)$.
- To study the behavior of the new equation $n(D)$, by varying the input parameters in the model.
- To fit previously published experimental data for the nonlinear dose response of various signals.

This paper is organized as follows. Section 2 describes the previously published delocalized transition model by Bowman and Chen [12]. Section 3 presents the derivation of the new analytical equation $n(D)$ for the dose response function of the dosimetric trap. Furthermore, the behavior of this new equation is studied by varying the physically meaningful parameters in the model. Section 4 discusses the combined effect of the irradiation and readout stages on superlinearity, within the context of the mixed order kinetics model (MOK). In section 5, experimental data for several dosimetric materials are fitted using the new dose response equation. Section 6 contains a summary and general discussion of the new dose response equation, and the paper concludes with the Appendix containing some of the mathematical details in the model by Bowman and Chen [12].

2. Competition during the irradiation stage: the model of Bowman and Chen [12]

In this section we consider the model of Bowman and Chen [12], which describes superlinear dose response as being a result of competition between two electron traps during the irradiation stage of a sample. Fig. 1 shows a schematic diagram of their two trap one recombination center model (2T1R), and the relevant electronic transitions during the irradiation of a sample. The differential equations governing the traffic of electrons between the two trapping levels, the recombination center and the conduction band (CB) and valence band (VB) in the 2T1R model are [1]:

$$\frac{dn_1}{dt} = A_1(N_1 - n_1)n_c, \tag{4}$$

$$\frac{dn_2}{dt} = A_2(N_2 - n_2)n_c, \tag{5}$$

$$\frac{dn_c}{dt} = X - A_1 n_c(N_1 - n_1) - A_2(N_2 - n_2)n_c - A_m m n_c, \tag{6}$$

$$\frac{dm}{dt} = -A_m m n_c + A_v(M - m)n_v, \tag{7}$$

$$m + n_v = n_1 + n_2 + n_c. \tag{8}$$

Here n_1 (cm^{-3}), n_2 (cm^{-3}) and m (cm^{-3}) are the concentrations of electrons in the two traps and of holes in recombination centers respectively, and N_1, N_2, M (cm^{-3}) are the total concentrations of the two trapping states and recombination center. n_c (cm^{-3}) and n_v (cm^{-3}) are respectively the concentrations of free electrons and holes. A_1 ($cm^{-3}s^{-1}$), A_2 (cm^3s^{-1}) are the trapping coefficient of electrons, A_m (cm^3s^{-1}) the recombination coefficient of electrons, and A_v (cm^3s^{-1}) is the trapping coefficient of holes in centers. X ($cm^{-3}s^{-1}$) is proportional to the dose-rate of excitation, and actually denotes the rate of production of electron-hole pairs by the excitation irradiation per unit volume per second. If the irradiation time is t, the dose received by the sample is $D = Xt$ (cm^{-1}). Eqs. (4) and (5) express the trapping of electrons from the conduction band into the two traps. Eqs. (6) and (7) describe the rate of change of the concentration of electrons in the CB and of holes in the recombination center, respectively. Eq. (8) is the charge neutrality condition, assuming initially empty traps and centers.

In this 2T1R model, the superlinear filling of the active trap N_1 can be described qualitatively as follows. At low doses the excitation fills both traps linearly, while at a critical dose the competing trap N_2 saturates, hence more electrons are made available to the trap of interest N_1. This

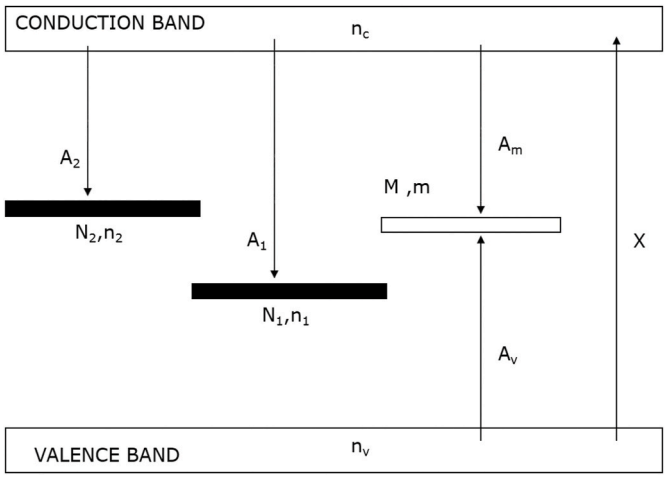

Fig. 1. The 2T1R model of Bowman and Chen [12], describing competition effects during the irradiation stage. Various electronic transitions are shown during the irradiation process. Transition X: Creation of electron-hole pairs by radiation. Transitions A_v and A_m: Trapping of holes and recombination of electrons at the recombination centers (RC). Transitions A_1, A_2: Trapping of electrons in the dosimetric and competitor trap.

causes a faster filling of this trap, with the transition region in the dose response curve above this critical dose appearing to be superlinear, before the dosimetric trap approaches saturation also.

The above set of differential equations cannot be solved analytically and one uses the quasi-equilibrium (QE) assumption, to transform them into a single differential equation. Specifically, Bowman and Chen [12] used the QE assumptions, and found the solutions $n_1(t)$ and $n_2(t)$ in terms of the following *implicit* functions for $D(n_1)$ and $n_2(n_1)$:

$$D = N_2\frac{A_m - A_2}{A_2}\left[\left(1-\frac{n_1}{N_1}\right)^{\frac{A_2}{A_1}} - 1\right] + \frac{A_1 - A_m}{A_1}n_1 - \frac{(N_1+N_2)A_m}{A_1}\ln\left(1-\frac{n_1}{N_1}\right) \tag{9}$$

$$n_2 = N_2\left\{1-\left(1-\frac{n_1}{N_1}\right)^{A_2/A_1}\right\} . \tag{10}$$

The first equation is a parametric equation in the form $D(n_1)$, in which one can enter any value of n_1/N_1 between 0 and 1, and evaluate numerically the corresponding dose D. Once the dose response function for the first trap $n_1(D)$ is obtained in this manner by using Eq. (9), the dose response function $n_2(D)$ of the second trap can be obtained from Eq. (10). These equations from the model by Bowman and Chen [12] are also derived in the Appendix Sections 7.1 and 7.2 of this paper, so that readers can refer to them easily.

Our goal in this paper is to bring these two parametric equations into the more useful analytical dose response forms $n_1(D)$ and $n_2(D)$.

In the next section, Eq. (9) is inverted and brought in the useful form $n_1(D)$, by using the Lambert function $W(x)$. Once $n_1(D)$ is obtained in analytical form, then $n_2(D)$ is also obtained analytically by substituting into Eq. (10).

3. Analytical equation for the dose response functions $n_1(D)$ and $n_2(D)$ of the two traps

In the derivation that follows, we designate n_1 as the concentration of trapped electrons in the competitor trap, and n_2 as the concentration of trapped electrons in the dosimetric trap of interest. This designation is opposite to that used by Bowman and Chen [12], who designated n_1, n_2 as the dosimetric and competitor trap respectively. The reason for this change in notation is so that a series expansion can be carried out in terms of the parameter A_2/A_1 in this paper, as will be shown below.

Starting with the term $(1-n_1/N_1)^{A_2/A_1}$ in Eq. (9), we write:

$$\left(1-\frac{n_1}{N_1}\right)^{A_2/A_1} = \left\{e^{\ln\left(1-\frac{n_1}{N_1}\right)}\right\}^{A_2/A_1} = e^{(A_2/A_1)\ln\left(1-\frac{n_1}{N_1}\right)} . \tag{11}$$

By assuming $A_2/A_1 \ll 1$, we carry out a series expansion for small A_2/A_1, by using the approximation $e^x \cong 1+x$:

$$\left(1-\frac{n_1}{N_1}\right)^{A_2/A_1} = e^{(A_2/A_1)\ln\left(1-\frac{n_1}{N_1}\right)} \cong 1 + (A_2/A_1)\ln\left(1-\frac{n_1}{N_1}\right) , \tag{12}$$

therefore

$$(1-n_1/N_1)^{A_2/A_1} - 1 \cong (A_2/A_1)\ln(1-n_1/N_1) . \tag{13}$$

Substituting Eq. (13) into Eq. (9), collecting terms and simplifying, we obtain:

$$-(A_2N_2 + A_mN_1)\ln(1-n_1/N_1) - N_1(A_m - A_1)(n_1/N_1) = DA_1 . \tag{14}$$

We now introduce the trap filling ratio parameter x:

$$x = n_1/N_1 , \tag{15}$$

so that Eq. (14) becomes:

$$-(A_2N_2 + A_mN_1)\ln(1-x) - N_1(A_m - A_1)x = DA_1 , \tag{16}$$

$$\ln(1-x) + \frac{N_1(A_m - A_1)}{A_2N_2 + A_mN_1}x = -\frac{DA_1}{A_2N_2 + A_mN_1} . \tag{17}$$

We note that this equation is of the general algebraic form:

$$\ln(a+bx) + cx = \ln d , \tag{18}$$

which has the analytical solution (see for example the websites dedicated to the Lambert function [13,14]):

$$x = \frac{1}{c}W\left[\frac{cd}{b}\exp\left(\frac{ac}{b}\right)\right] - \frac{a}{b} . \tag{19}$$

By substituting $a = 1$, $b = -1$, $c = \frac{N_1(A_m - A_1)}{A_2N_2 + A_mN_1}$, $\ln d = -\frac{DA_1}{A_2N_2 + A_mN_1}$ or $d = \exp\left(-\frac{DA_1}{A_2N_2 + A_mN_1}\right)$, we obtain:

$$\frac{n_1}{N_1} = 1 + \frac{1}{c}W\left[-c\exp(-c)\exp\left(\frac{-DA_1}{A_2N_2 + A_mN_1}\right)\right] , \tag{20}$$

$$\frac{n_1}{N_1} = 1 - \frac{1}{B}W[B\exp(B)\exp(-D/D_c)] , \tag{21}$$

where we defined the two constants B, D_c such that:

$$B = -c = \frac{N_1(A_1 - A_m)}{A_2N_2 + A_mN_1} , \tag{22}$$

$$D_c = \frac{A_2N_2 + A_mN_1}{A_1} . \tag{23}$$

Equation (21) is the desired analytical expression for the dose response function $n_1(D)$ of the first trap, which is designated the competitor trap. The dose response function $n_1(D)/N_1$ in this rather simple equation depends on only two parameters, the constants B and D_c, which are given by Eqs. (22) and (23) in terms of the 5 parameters A_m, A_1, A_2, N_1, N_2 in the model. The parameter D_c has the same dimensions at the irradiation dose D, so that the ratio D/D_c in Eq. (21) is dimensionless. As seen from the definition in Eq. (22), the parameter B is also dimensionless.

By substituting Eq. (21) in Eq. (10), we obtain:

$$\frac{n_2}{N_2} = 1 - \left(\frac{1}{B}W[B\exp(B)\exp(-D/D_c)]\right)^{A_2/A_1} . \tag{24}$$

This is the new desired analytical expression for the dose response function $n_2(D)/N_2$ of the second trap, which is designated the *dosimetric* trap. The assumptions in deriving Eq. (24) and Eq. (21) are the QE conditions, and the additional condition $A_2/A_1 < 1$, which allowed the series expansion of Eq. (11) for small values of A_2/A_1.

It is noted that Eqs. (21) and (24) are otherwise completely general, and that the overall dose response function in this model will depend on the numerical values of only three parameters appearing in these equations: B, D_c, A_2/A_1.

Fig. 2a shows a plot of the dose responses n_1/N_1 and n_2/N_2, as a function of the normalized dimensionless dose D/D_c, using Eqs. (21) and (24). The numerical values of the parameters are $A_2/A_1 = 0.1 < 1$ and $B = 10$. Fig. 2b shows the same data in a loglog scale, and the superlinear behavior is clearly seen. As the competitor trap approaches saturation ($n_1/N_1 \to 1$), the dose response of the dosimetric trap n_2/N_2 becomes superlinear. With this set of parameters, the series approximation used in the derivation is expected to be valid at all doses.

The initial short linear range in the curve n_2/N_2 in Fig. 2a is followed by a range of superlinearity, which eventually becomes sublinear on its way to saturation.

Fig. 3a shows a simulation of the dose response function $n_1(D)/N_1$ of the competitor trap, as a function of the normalized dose D/D_c. In this simulation the ratio A_2/A_1 is kept constant, while varying the

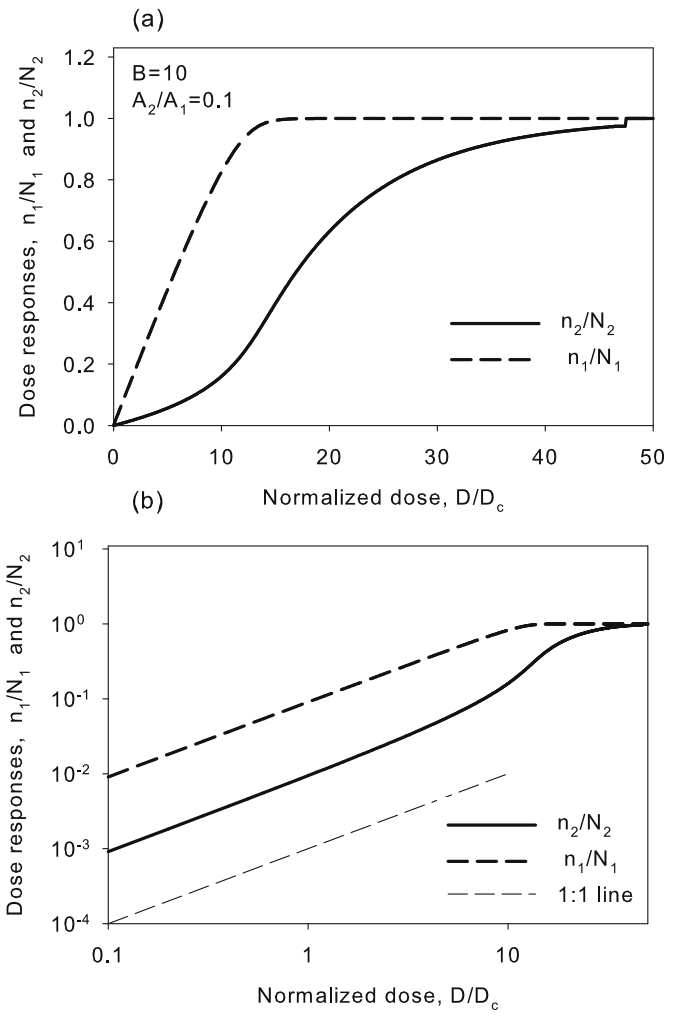

Fig. 2. (a) Plot of the dose responses n_1/N_1 and n_2/N_2, as a function of the normalized dose D/D_c, using Eqs. (21) and (24) and the model parameters $A_2/A_1 = 0.1 < 1$ and $B = 10$. (b) The same data as in (a), on a loglog scale. As the competitor trap (n_1/N_1) approaches saturation, the dose response function of the dosimetric trap n_2/N_2 becomes superlinear.

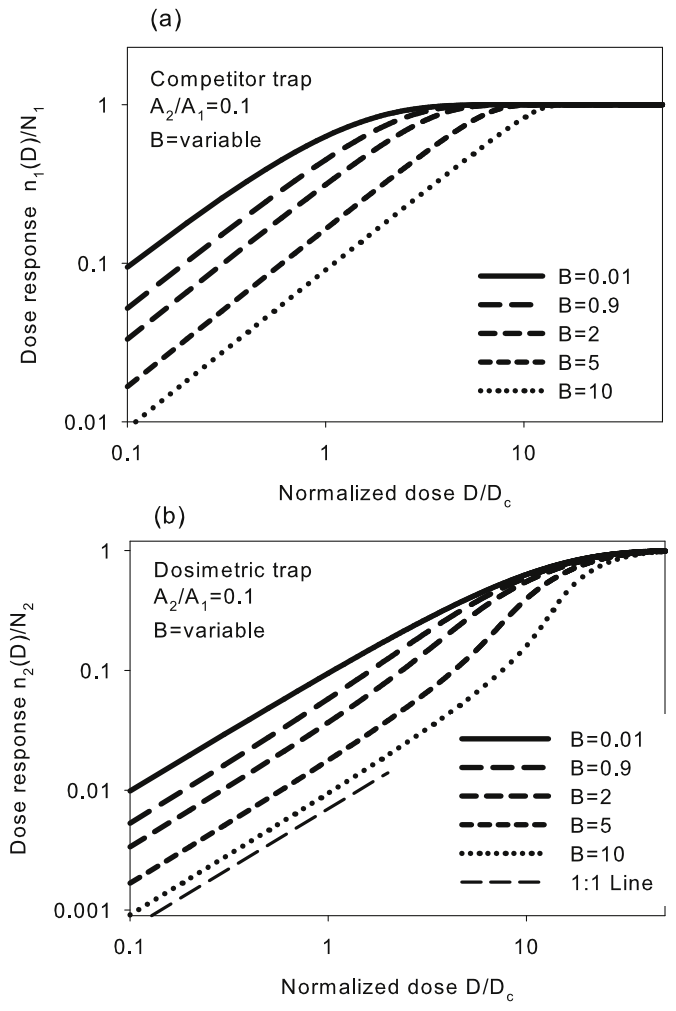

Fig. 3. (a) dose response function $n_1(D)/N_1$ of the competitor trap, as a function of the normalized dose D/D_c. The ratio A_2/A_1 is kept constant, while varying the dimensionless parameter B in the model. (b) The corresponding dose response function $n_2(D)/N_2$ of the dosimetric trap. As the competitor trap approaches saturation in (a), the behavior of the dosimetric trap in (b) becomes superlinear.

dimensionless parameter B in the model. Fig. 3b shows the corresponding dose response function $n_2(D)/N_2$ of the dosimetric trap. As the competitor trap approaches saturation in (a), the behavior of the dosimetric trap in (b) becomes superlinear. The curves for $B = 5, 10$ in this figure show superlinear behavior, while the curve with $B < 1$ shows the typical linear-to-saturation behavior.

Fig. 4a shows the dose response function $n_2(D)/N_2$ of the dosimetric trap on a loglog scale, as a function of the normalized dose $D/\ D_c$. The dimensionless parameter B is kept constant at $B = 5 > 1$, while varying the ratio A_2/A_1 in the model. The dose response function in (a) is clearly superlinear when $A_2/A_1 < 1$, and becomes linear when $A_2/\ A_1 > 1$.

Fig. 4b shows the same simulation as in Fig. 4a, for a value of the parameter $B = 0.9 < 1$. No superlinearity phenomena are observed in (b).

As could have been expected, the simulations show that the behavior of the dose response function $n_2(D)/N_2$ depends on the value of the parameters B and A_2/A_1. The simulations in Figs. 3 and 4 show that when *both* of the two conditions $B > 1$ and $A_2/A_1 < 1$ are satisfied, the dose response function $n_2(D)$ of the dosimetric trap is superlinear. When only one of these conditions is satisfied, the dose response is similar to the behavior of the traps in the OTOR model, i.e. a linear-sublinear-saturation behavior. This type of behavior was studied in detail in the recent OTOR paper by Pagonis et al. [9].

The new analytical equation developed in this section can be used to fit experimental dose response curves for ESR and OA data, since these signals are directly proportional to the dose response function $n_2(D)$ of the dosimetric trap. This raises the important question whether the new equations can also be used to fit experimental TL or OSL dose response curves, which are affected by *both* the irradiation and the readout stages in a luminescence experiment.

As discussed in Pagonis et al. [9], when first order kinetics is prevalent during the readout stage, the dose response curves for the excitation and readout stage will be identical. In such cases, the analytical Eq. (24) developed in this paper can be used to analyze experimental ESR, OA, TL and OSL data. It is important to keep in mind that the vast majority of TL dosimetric materials exhibit first order kinetics processes, and that there have been very few reports of non-first order kinetics behavior. This overwhelming prevalence of first order kinetics in nature, has been explained by Pagonis and Kitis [16], by simulating TL glow curves in the presence of many competitors. These authors showed that

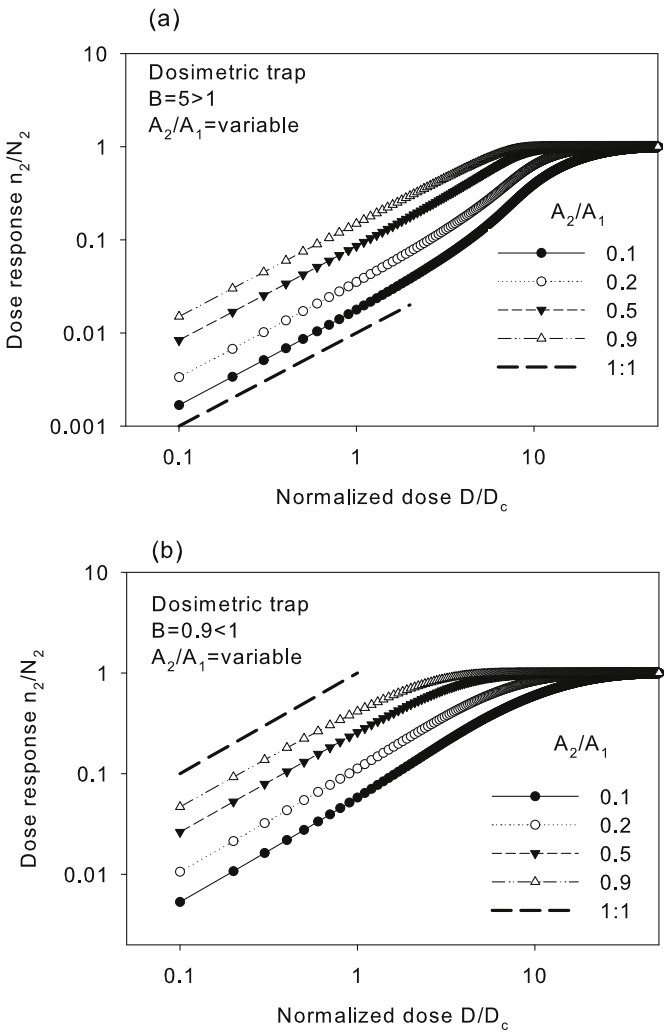

Fig. 4. (a) dose response function $n_2(D)/N_2$ of the dosimetric trap on a loglog scale, as a function of the normalized dose D/D_c. The dimensionless parameter B is kept constant at $B = 5 > 1$, while varying the ratio A_2/A_1 in the model. The dose response function in (a) is clearly superlinear when $A_2/A_1 < 1$. (b) The same simulation as in (a), for $B = 0.9 < 1$. No superlinearity phenomena are observed in (b).

the physical origin of first order kinetics is the presence of competitors in a dosimetric material. As the number of competitors increases, the kinetic order tends towards first order.

In the next section we discuss the combined effect of the irradiation and readout stages on the superlinearity of the dose response curves, before we proceed in section 5 to fit experimental ESR, OA, TL and OSL data.

4. The effect of the readout stage on a superlinear dose response

Chen et al. [15] discussed the two types of models usually employed for explaining the superlinear dose dependence of luminescence signals. The first type of model involves competition during excitation between trapping states, which causes the filling of the relevant trap or center to be superlinear. This is the type of model which was described in Fig. 1, and was discussed in the previous section.

The second type of model deals with competition during the thermal or optical readout stage, producing a TL and OSL signal correspondingly. The readout stage may also result in a strong superlinearity, even if the filling of the trap and center in question are linear with the dose. Chen et al. [15] showed that both the irradiation stage and readout stage can cause superlinearity in multitrap models, resulting in a very steep superlinear behavior. These authors showed that the readout stage introduces an additional amount of superlinearity.

As an example of superlinearity occurring during both the irradiation and readout stages, in this section we consider the special case of mixed order kinetics (MOK). As discussed in the recent review paper by Kitis et al. [33] the luminescence intensity during the *readout* stage of the MOK model is described by the differential equation ([33]):

$$I(t) = -\frac{dn_2}{dt} = \frac{A_m}{N_2 A_1}\, p(t)\, n_2\, (n_2 + N_1)\,. \tag{25}$$

In this expression, as in the rest of this paper, (n_1, N_1) and (n_2, N_2) denote the concentrations of the competitor trap and dosimetric trap, respectively. This is the general differential equation for the mixed-order kinetics (MOK) model, which is the sum of the two terms, a linear term in the concentration n_2, and a quadratic term $(n_2)^2$, corresponding to first and second order kinetics respectively. Furthermore, when the total concentration of competitors N_1 becomes larger than the concentration of dosimetric traps n_2 so that $N_1 \gg n_2$, then Eq. (25) becomes a first order kinetics equation.

This can be rewritten in the more convenient form:

$$I = \frac{A_m N_2}{A_1}\, p(t)\, \frac{n_2}{N_2} \left(\frac{n_2}{N_2} + \frac{N_1}{N_2}\right). \tag{26}$$

In the 2T1R model, the trap filling ratio n_2/N_2 at the end of the irradiation stage is given by the analytical Eq. (24):

$$\frac{n_2}{N_2} = 1 - \left(\frac{1}{B} W[B\exp(B)\exp(-D/D_c)]\right)^{A_2/A_1}. \tag{27}$$

By combining Eqs. (26) and (27), we obtain the following new analytical expression, which contains the superlinear dose response due to *both* the irradiation and readout stages in the MOK model:

$$I = k\left\{1 - \left(\frac{1}{B} W[z]\right)^{A_2/A_1}\right\} \left(1 - \left(\frac{1}{B} W[z]\right)^{A_2/A_1} + \frac{N_1}{N_2}\right), \tag{28}$$

$$z = B\exp(B)\exp(-D/D_c)\,. \tag{29}$$

where k is a constant. Fig. 8a shows the plot of Eq. (28) for the MOK model, by varying the ratio N_1/N_2 and using the same model parameters $B = 10$, $A_2/A_1 = 0.1$ as in Fig. 2.

As discussed previously by Chen et al. [15], the readout stage introduces an additional amount of superlinearity, due to the presence of the additional quadratic term (n_2/N_2). In the MOK model, Eq. (28) shows that the extra amount of superlinearity depends on the parameter N_1/N_2. This is seen clearly in Fig. 8b, which shows the supralinearity index $f(D)$, calculated for the dose response curves shown in (a). As the parameter N_1/N_2 increases in the direction of the arrow, the corresponding supralinearity index $f(D)$ decreases in a systematic manner.

In conclusion, when a dosimetric material exhibits first order kinetics behavior during the readout stage, then one can use in principle the new analytical Eq. (24) to fit OA, ESR, TL and OSL dose response data.

On the other hand, when a dosimetric material exhibits non-first order kinetic behavior, it may be possible to use Eq. (28) to fit the corresponding TL and OSL data; this equation contains the superlinearity effects resulting from both the irradiation and readout stages, at least within the MOK model presented here.

However, one must keep in mind that as pointed out by Chen et al. [15], it is in general difficult to separate the superlinearity effects produced during the irradiation stage, from those due to the readout stage.

5. Fitting of experimental data using the new analytical Eq. (24)

In this section we fit experimental ESR, OA and TL data by using the new analytical Eq. (24). The best fit parameters for each of the examples in this section are given in Table 1. The values of B, A_2/A_1 and D_c for the

Table 1
Summary of the best fitting values B,A_2/A_1, D_c obtained by using Eq. (24) to fit the experimental data in Figs. 5–7.

Figure in this paper	Type of data	B	A_2/A_1	D_c (Gy)
5	ESR	3.22	0.020	266.7
5	TL	3.56	0.024	94.3
5	OA (α)	3.95	0.028	434.8
6 (600°C)	TL	13.9	0.015	2.18
6 (700°C)	TL	9.67	0.039	2.39
6 (800°C)	TL	7.50	0.716	8.0
6 (900°C)	TL	4.35	0.0086	0.25
7 (Crystal 1)	TL	1.26	0.21	0.24
7 (Crystal 2)	TL	6.87	0.030	0.051
7 (Crystal 4)	TL	2.89	0.10	0.12

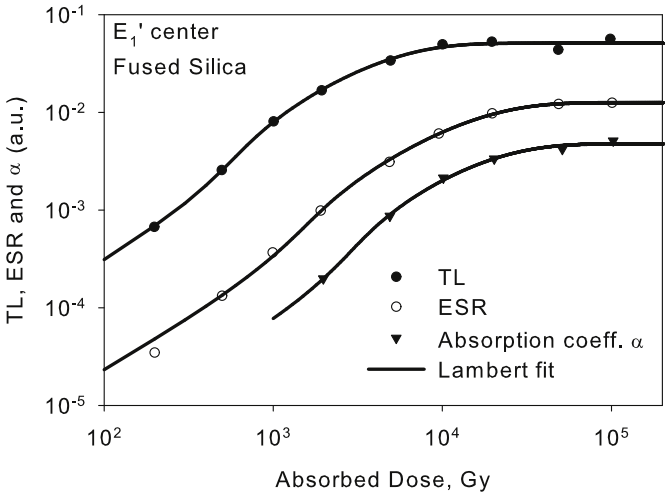

Fig. 5. Superlinear dose dependence of the E'_1 center concentration (ESR), TL and OA signals in fused silica [17]. The growth of the E'_1 center concentration was measured using ESR spectroscopy, and is correlated with the growth of the optical E-band absorption, and with TL measurements of the 415 °C glow peak. The solid lines represent the fits using Eq. (21), with the best fit parameters given in Table 1.

least squares fits in Figs. 5–7 are summarized in Table 1. The data in this Table shows that the conditions $B > 1$ and $A_2/A_1 < 1$ are indeed satisfied in all cases. This is an indication that using Eq. (18) to fit the luminescence intensity is consistent with the assumption of first order kinetics.

Fig. 5 shows ESR,TL and optical absorption data for fused silica, by Wieser et al. [17]. The E'_1 center is observed in all forms of quartz and silica, however these authors found an unexpected superlinear dose dependence of the E'_1 center in fused silica. Previously a superlinear dose response in quartz had been observed with TL, but not with optical or ESR spectroscopy. They reported a superlinear increase of the E'_1 center concentration by irradiation, and compared their results with the growth of the correlated optical E-band absorption, and with TL measurements which showed a correlation of the 415°C glow to the E'_1 center. The solid lines in Fig. 5 represent least squares fits using the analytical Eq. (24).

The Lambert-based equation in this paper describes well all three types of dose responses for this material: ESR, TL and OA. The values of the parameters of B and A_2/A_1 in Table 1 are very similar for the ESR, TL and OA data in Fig. 5, indicating a strong correlation between these three types of signals.

In the example of Fig. 5 the nature of the trap is known (i.e. the E'_1 center in fused silica), while the nature of the competitor is unknown.

A luminescence signal which has been studied extensively is the 110°C TL peak in different types of natural and synthetic quartz. This TL peak has been shown in many studies to follow first order kinetics, and we would therefore expect that its dose response would be described by Eq. (24).

Fig. 6 shows data from Fig. 2A of Charitidis et al. [18]. These authors studied synthetic quartz samples which were annealed at several temperatures in the range 600–900°C before measuring the dose response of the 110°C TL peak in quartz. Fig. 6 shows the dependence of the superlinear behavior on the firing temperature. The experimental data are fitted with the new Lambert equation, with the best fits shown as solid lines. It is concluded that the new analytical Eq. (24) describes well the variation of the superlinear dose response with the annealing temperature in synthetic quartz.

It is interesting to note that the values of the parameters of B and A_2/A_1 in Table 1 vary in a systematic manner for the quartz annealed at 600-700-800°C, while the best fit parameters for quartz annealed at 900°C do not follow the same systematic pattern. The cause for this disagreement is not clear, and could be an artifact of the fitting procedure.

In the example of Fig. 6 the nature of the trap and centers in some types of quartz have been identified. For example, the experimental work by Yang and McKeever [19] showed that the 110°C TL peak in crystalline quartz is due to the recombination of electrons released from $(GeO_4)^-$ centers with holes trapped at $(AlO_4)^0$ centers and at $(H_3O_4)^0$ centers. The competitor traps and centers in quartz are commonly assumed to be one of the deep electron traps or centers corresponding to the higher temperatures in the glow curve (see for example Chapter 9 in Ref. [1], for comprehensive quartz models available in the literature).

As a third example of fitted experimental data, Fig. 7 shows curves 1-2-4 from Nikiforov et al. [20], their Fig. 7. These authors measured the TL dose response characteristics of anion deficient aluminum oxide single crystals. Crystals (1, 2) in Fig. 7 correspond to two samples with low initial sensitivity, and crystal (4) to a sample with high initial sensitivity to beta radiation. The heating rate for these measurements was 6 K/s. Once more, the new analytical Eq. (24) describes well the variation of the superlinear dose response for the different samples of anion deficient aluminum oxide crystals.

In the example of Fig. 7 and as discussed in the experimental work by Nikiforov et al. [20], the luminescence mechanism includes the main dosimetric trap, a competing deep electron trap, and the luminescence center which is known to represent an F^+ center in anion deficient aluminum oxide. The TL intensity in the dominant emission band at 420 nm is associated with the capture of delocalized electrons by F^+ centers.

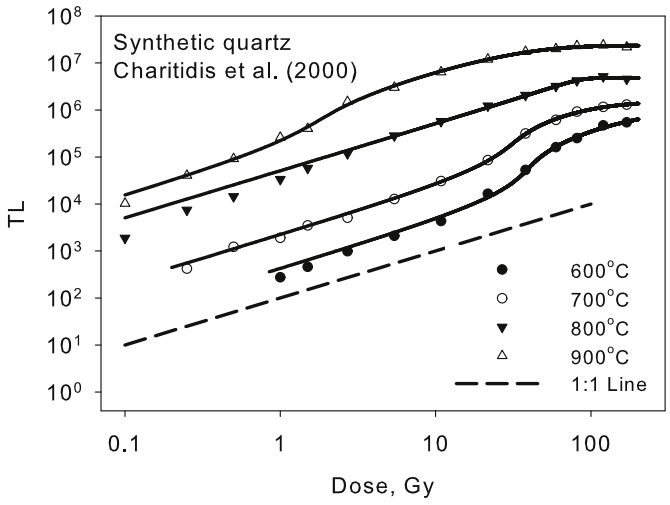

Fig. 6. Data from Fig. 2A of Charitidis et al. [18], showing the superlinear behavior of the 110°C TL peak in fired synthetic quartz. The samples were annealed at several temperatures in the range 600–900 °C. The experimental data are fitted with the new Lambert Eq. (21), (solid lines), with the best fit parameters given in Table 1.

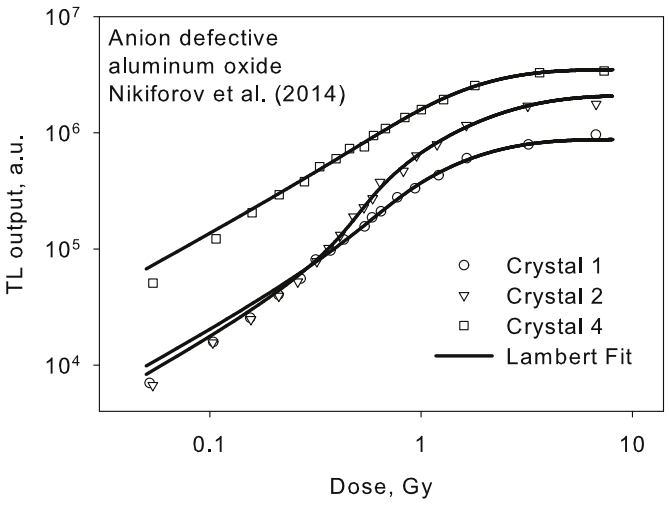

Fig. 7. Curves 1-2-4 from Nikiforov et al. [20], showing dose characteristics of 3 different anion deficient aluminum oxide single crystals (their Fig. 7). Crystals 1 and 2 have low initial sensitivity to irradiation, while crystal 4 has high initial sensitivity. The heating rate is 6 K/s. The experimental data are fitted with the new Lambert Eq. (21), (solid lines), with the best fit parameters given in Table 1.

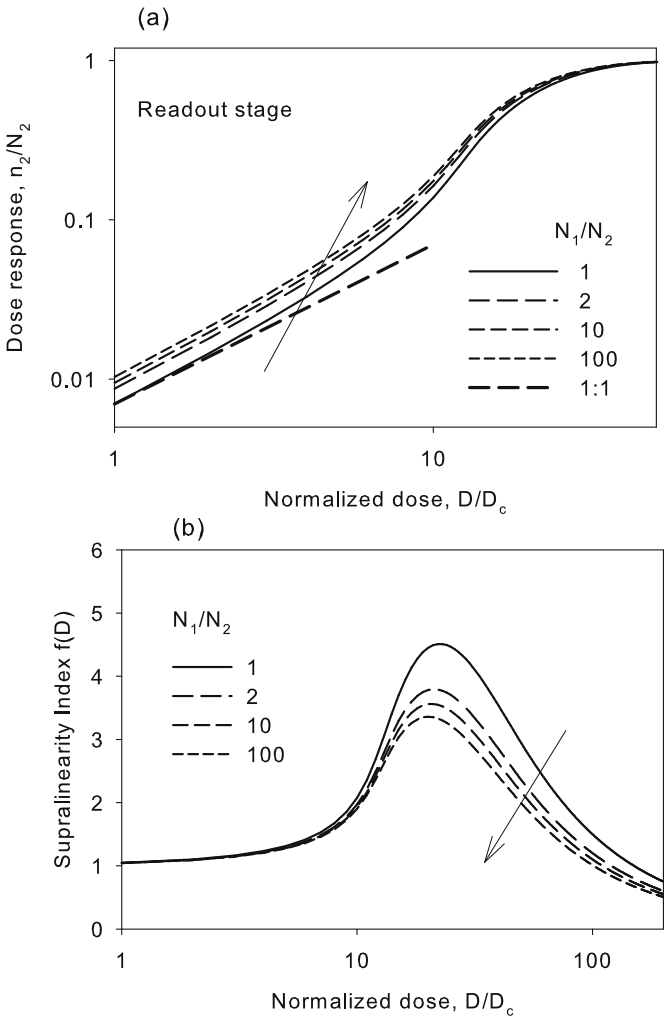

Fig. 8. (a) The effect of the parameter N_1/N_2 on the superlinear dose response of the TL signal in the MOK model (readout stage). (b) The supralinearity index $f(D)$ calculated for the dose response curves shown in (a).

The competitor traps are commonly assumed to be one of the deep electron traps or centers corresponding to the higher temperatures observed in the glow curve.

The actual luminescence mechanism in the above three examples are of course much more complex than the simple model proposed in this paper. However it is very encouraging that the superlinear behavior of the ESR, OA and TL signals in these dosimetric materials can be described well by the new analytical Eq. (24).

6. Discussion, summary and conclusions

We conclude this paper with a general discussion of the nonlinear dose response of dosimetric materials. The dose dependence of TL, OSL and ESR signals in the high dose region exhibits many different types of nonlinear dependence.

If we consider only the very simple OTOR model, a linear-saturation behavior is always expected. This case has been studied in detail in Pagonis et al. [9], who found the analytical equation for the trap filling ratio n/N:

$$\frac{n(D)}{N} = 1 - \frac{1}{R-1}\, W[(R-1)\exp(R-1-D/D_c)]\,. \tag{30}$$

In this OTOR model, the function $n(D)/N$ depends only on two parameters, i.e. on the retrapping ratio R and on the dose scaling constant D_c. The parameter D_c has the same units as the dose D, and depends on the physical properties of the material.

In real materials several trapping states and recombination centers exist, which take part in the irradiation and readout stages. The effects of competition can explain a wealth of different dose responses associated with TL, OSL, ITL, OA and ESR signals. As far as superlinear dose dependence is concerned, it has been shown that competition during excitation can yield one kind of behavior, while competition during read-out yields another kind of dependence. Simulations have also shown the combined effect of both kinds of competition (see for example [1]). In this paper it was shown that in the 2T1R model, the superlinear dose response function can be described by the analytical equation:

$$\frac{n_2}{N_2} = 1 - \left(\frac{1}{B} W[B\exp(B)\exp(-D/D_c)]\right)^{A_2/A_1}\,. \tag{31}$$

In this 2T1R model, the function $n_2(D)/N_2$ depends on three parameters, i.e. on the dimensionless constant B, on the ratio of trapping coefficients A_2/A_1 of the two competing traps, and on the dose scaling constant D_c. The parameter D_c has the same units as the dose D, and the other two parameters B, A_2/A_1 are dimensionless.

As discussed in Section 4, when a dosimetric material exhibits non-first order kinetic behavior, it may be possible to use the following analytical equation to fit the corresponding TL and OSL data:

$$I = k\left\{1 - \left(\frac{1}{B} W[z]\right)^{A_2/A_1}\right\}\left(1 - \left(\frac{1}{B} W[z]\right)^{A_2/A_1} + \frac{N_1}{N_2}\right)\,, \tag{32}$$

$$z = B\exp(B)\exp(-D/D_c)\,. \tag{33}$$

This equation was developed within the MOK model, and contains superlinearity effects resulting from both the irradiation and readout stages in a TL/OSL experiment.

By using the analytical equations developed in this paper, it is possible to develop new analytical equations for the superlinearity index $g(D)$, as well as for the supralinearity index $f(D)$. These results will be presented elsewhere due to their algebraic complexity, and they will also be compared with additional experimental data in the literature.

In the literature one also finds two alternative modeling approaches to the analytical equations and model presented in this paper. These are the track structure theory (TST), and the unified interaction model (UNIM). TST was introduced by Katz and collaborators in the 1960s [21–25], and is a model based on statistical considerations involving the

cumulative Poisson distributions for a single and multiple hit interactions occurring during irradiation of a sample. The UNIM model is based on a combination of localized and delocalized recombination mechanisms, which are prevalent at different dose regimes [26,27].

The advantages of the analytical equation developed in this paper are: the Lambert-based equation is simple, it contains physically meaningful parameters, it can be very easily adopted for various software, and can be used on an empirical basis to describe superlinear behavior of ESR, TL, OSL and OA data. An extensive application of the new Lambert Eq. (24) to describe published experimental data for these different types of signals will be presented in a future publication.

CRediT authorship contribution statement

Vasilis Pagonis: Conceptualization, Methodology, Software, Writing - review & editing. **George Kitis:** Conceptualization, Methodology, Software, Writing - review & editing. **Reuven Chen:** Conceptualization, Methodology, Software, Writing - review & editing.

Declaration of competing interest

The authors declare that they have no known competing financial interests or personal relationships that could have appeared to influence the work reported in this paper.

Appendix

In this Appendix we reproduce the analytical considerations in the model by Bowman and Chen [12], for easy reference. Specifically we derive Eqs. (9) and (10), which are the starting points of the analytical evaluations in this paper.

Derivation of Eq. (10) in this paper

We first evaluate n_1 as a function of n_2. From equations (4) and (5):

$$\frac{dn_2}{A_2(N_2-n_2)}=\frac{dn_1}{A_1(N_1-n_1)} \ . \tag{34}$$

Integrating the two sides from $n_2^{'}=0$ to n_2 , and from $n_1^{'}=0$ to n_1 respectively:

$$\frac{1}{A_2}\ln\left(\frac{N_2-n_2}{N_2}\right)=\frac{1}{A_1}\ln\left(\frac{N_1-n_1}{N_1}\right) \ , \tag{35}$$

$$\ln\left(\frac{N_2-n_2}{N_2}\right)=\ln\left\{\left(\frac{N_1-n_1}{N_1}\right)^{A_2/A_1}\right\} \ , \tag{36}$$

$$1-\frac{n_2}{N_2}=\left(1-\frac{n_1}{N_1}\right)^{A_2/A_1} \ , \tag{37}$$

$$n_2=N_2\left\{1-\left(1-\frac{n_1}{N_1}\right)^{A_2/A_1}\right\} \ . \tag{38}$$

This is Eq. (10) in this paper.

Derivation of Eq. (9) in this paper.

Starting from the charge conservation Eq. (8), and assuming QE conditions $n_c \ll n_1+n_2$ and $n_v \ll m$ we obtain:

$$m \simeq n_1+n_2 \ . \tag{39}$$

Substituting n_2 from Eq. (38):

$$m \simeq n_1+n_2=n_1+N_2\left\{1-\left(1-\frac{n_1}{N_1}\right)^{A_2/A_1}\right\} \ . \tag{40}$$

Using the QE condition $dn_c/dt \cong 0$ in Eq. (6), we obtain:

$$n_c=\frac{X}{A_m m+A_1(N_1-n_1)+A_2(N_2-n_2)} \ . \tag{41}$$

Substituting this value of n_c in Eq. (4):

$$\frac{dn_1}{dt}=A_1(N_1-n_1)\frac{X}{A_m m+A_1(N_1-n_1)+A_2(N_2-n_2)} \ , \tag{42}$$

$$\frac{dn_1}{A_1(N_1-n_1)}\left[A_m m+A_1(N_1-n_1)+A_2(N_2-n_2)\right]=X dt \ . \tag{43}$$

Substituting the value of $m=n_1+n_2$ from Eq. (40):

$$\frac{dn_1}{A_1(N_1-n_1)}\left[A_m(n_1+n_2)+A_1(N_1-n_1)+A_2(N_2-n_2)\right]=X dt \ , \tag{44}$$

$$\frac{dn_1}{A_1(N_1-n_1)}\left[n_1(A_m-A_1)+n_2(A_m-A_2)+A_1N_1+A_2N_2\right]=X dt \ . \tag{45}$$

Substituting the value of n_2 from Eq. (38):

$$\frac{dn_1}{A_1(N_1-n_1)}\left[n_1(A_m-A_1)+N_2\left\{1-\left(1-\frac{n_1}{N_1}\right)^{A_2/A_1}\right\}(A_m-A_2)+\right.$$

$$\left.+A_1N_1+A_2N_2\right]=Xdt\ . \tag{46}$$

The two sides of this differential equation for $n_1(t)$ can now be integrated with the initial condition $n_1(0)=0$ at time $t=0$, to obtain:

$$D=N_2\frac{A_m-A_2}{A_2}\left[\left(1-\frac{n_1}{N_1}\right)^{\frac{A_2}{A_1}}-1\right]+\frac{A_1-A_m}{A_1}n_1-\frac{(N_1+N_2)A_m}{A_1}\ln\left(1-\frac{n_1}{N_1}\right). \tag{47}$$

where $D=Xt$ represents the dose received by the sample. This is Eq. (9) in the paper by Bowman and Chen [12], and also Eq. (9) in this paper.

Appendix A. Supplementary data

Supplementary data to this article can be found online at https://doi.org/10.1016/j.jlumin.2020.117553.

References

[1] R. Chen, V. Pagonis, Thermally and Optically Stimulated Luminescence: A Simulation Approach, Wiley and Sons, Chichester, 2011.
[2] E.G. Yukihara, S.W.S. McKeever, Optically Stimulated Luminescence: Fundamentals and Applications, Wiley, Chichester, 2011.
[3] R. Chen, S.W.S. McKeever, Theory of Thermoluminescence and Related Phenomena, World Scientific, 1997.
[4] S.W.S. McKeever, Thermoluminescence of Solids, Cambridge University Press, Cambridge, 1985.
[5] R. Chen, S.W.S. McKeever, Characterization of nonlinearitiesin dose dependence of thermoluminescence, Radiat. Meas. 23 (1994) 667–673, 1994.
[6] Y.S. Horowitz, The theoretical and microdosimetric basis of thermoluminescence and applications to dosimetry, Phys. Med. Biol. 26 (5) (1981) 765.
[7] E.F. Mische, S.W.S. McKeever, Mechanisms of supralinearity in Lithium fluoride thermoluminescence dosemeters, Radiat. Protect. Dosim. 29 (1989) 159–175.
[8] J.L. Lawless, R. Chen, V. Pagonis, Sublinear dose dependence of thermoluminescence and optically stimulated luminescence prior to the approach to saturation level Radiat, Meas 44 (2009) 606–610.
[9] V. Pagonis, G. Kitis, R. Chen, A new analytical equation for the dose response of dosimetric materials, based on the Lambert W function, J. Lumin. 225 (2020) 117333.
[10] R.M. Corless, G.H. Gonnet, D.G.E. Hare, D.J. Jeffrey, D.E. Knuth, On the Lambert W function, Adv. Comput. Math. 5 (1996) 329–359.
[11] S.R. Valluri, D.J. Jeffrey, R.M. Corless, Some applications of the Lambert W function in physics canad, J. Phys. 78 (2000) 823–831.
[12] S.G.E. Bowman, R. Chen, J. Lumin. 18/19 (1979) 345–348.
[13] E.W. Weisstein, Lambert W-function." from MathWorld–A wolfram web resource. http://mathworld.wolfram.com/LambertW-Function.html. (Accessed 3 March 2020).
[14] K. Briggs, W-ology, or, some exactly solvable growth models. http://keithbriggs.info/W-ology.html. (Accessed 3 March 2020).
[15] R. Chen, G. Fogel, C.K. Lee, A new look at the models of the superlinear dose dependence of thermoluminescence, Radiat. Protect. Dosim. 65 (1996) 63–68, 1996.
[16] V. Pagonis, G. Kitis, Prevalence of first order kinetics in thermoluminescence materials: an explanation based on multiple competition processes, Phys. Status Solidi B (2012) 1–12, https://doi.org/10.1002/pssb.201248082, 2012.
[17] A. Wieser, Y. Göksu, D.F. Regulla, A. Waibel, Unexpected superlinear dose dependence of the E′$_1$center in fused silica, Int. J. Radiat. Appl. lnstrum. , Part D . Nucl. Tracks Radiat. Meas. 18 (No 1/2) (1991) 175–178.
[18] C. Charitidis, G. Kitis, C. Furetta, S. Charalambous, Superlinearity of synthetic quartz: dependence on the firing temperature, Nucl. Instrum. Methods Phys. Res. B 168 (2000) 404–410.
[19] X.H. Yang, S.W.S. McKeever, The predose effect in crystalline quartz, J. Phys. D Appl. Phys. 23 (1990) 237–244.
[20] S.V. Nikiforov, V.S. Kortov, M.G. Kazantseva, Simulation of the superlinearity of dose characteristics of thermoluminescence of anion deficient aluminum oxide, Phys. Solid State 56 (3) (2014) 554–560.
[21] R. Katz, Track structure theory in radiobiology and radiation protection Nucl, Track Det 2 (1978) 1–28.
[22] J.J. Butts, R. Katz, Theory of RBE of heavy ion bombardment of dry enzymes and viruses, Radiat. Res. 30 (1967) 855–871.
[23] R. Katz, Track structure theory in radiobiology and in radiation detection, Nucl. Track Detect. 2 (1–28) (1978).
[24] R. Katz, S.C. Sharma, M. Homayoonfar, The structure of particle tracks, in: F. H. Attix (Ed.), Topics in Radiation Dosimetry, Academic press, New York (USA), 1972, p. 317. Supplement 1.
[25] M.P.R. Waligorski P. Olko, P. Bilski, M. Budzanowski T, Niewiadomski Dosimetric characteristic of LiF:Mg,Cu,P phosphors - a track structure interpretation, Radiat. Protect. Dosim. 47 (1993) 53–58.
[26] Y.S. Horowitz, Theory of thermoluminescence gamma dose response: the unified interaction model, Nucl. Instrum. Meths B 184 (2001) 68–84.
[27] Y.S. Horowitz, Y. Belaish, L. Oster, Theories of TL systems: failures, successes, conflicts, trends: insights into the possible future materials and techniques, Radiat. Protect. Dosim. 119 (2006) 124–129.
[33] G. Kitis, G.S. Polymeris, V. Pagonis, Stimulated luminescence emission: from phenomenological models to master analytical equations, Appl. Radiat. Isot. 153 (2019) 108797.